Spin-isospin nuclear responses with hadronic probes

W. M. Alberico,[a] A. De Pace,[a] M. Ericson,[b] Mikkel B. Johnson,[c] and A. Molinari[a]
[a]*Dipartimento di Fisica Teorica dell'Università di Torino, 10125 Torino, Italy and Istituto Nazionale di Fisica Nucleare, Sezione di Torino, Torino, Italy*
[b]*Université C. Bernard Lyon I, 69621 Villeurbanne, France and European Organization for Nuclear Research, Geneva, Switzerland*
[c]*Los Alamos National Laboratories, Los Alamos, New Mexico 87545*
(Received 28 September 1987)

We develop a random-phase approximation theory of the spin-isospin nuclear surface response, suitable for the interpretation of recent experiments of polarized (p,p′) and charge exchange (^{3}He,t) reactions. The present approach extends our previous treatment of the volume responses, which was quite successful in accounting for inelastic electron scattering data. Its crucial ingredient is a vertex function which localizes the probe-target interaction on the surface region of the nucleus. Our results compare rather successfully with both the (p,p′) and (^{3}He,t) experiments, although some difficulties remain to be overcome. Indeed, we predict a ratio between the spin-longitudinal and the spin-transverse nuclear responses still somewhat larger than the measured value. Concerning the charge-exchange (^{3}He,t) reaction, we qualitatively account for the progressive softening of the peak of the cross section at large momentum transfer, thus confirming the role of the pion in nuclear structure. We tentatively ascribe the remaining discrepancies with the (^{3}He,t) data to relativistic kinematics effects.

I. INTRODUCTION

The problem of the role of the pion in the nuclear spin-isospin ($\sigma\tau$) response is still an open one. Indeed it has been argued[1] that the attractive particle-hole (p-h) force provided by the pion exchange should induce an enhancement and a softening, with respect to the free response, of the spin longitudinal ($\boldsymbol{\sigma}\cdot\mathbf{q}$) nuclear response R_L in the quasi-elastic peak (QEP) region for momenta of the order of about three pion masses μ_π. The spin transverse ($\boldsymbol{\sigma}\times\mathbf{q}$) response ($R_T$) instead should be unaffected by the pion in the nuclear matter limit and the corresponding force, being of much shorter range, remains repulsive up to quite large momenta (>2 fm^{-1}), thus quenching and hardening the QEP. Therefore, the pion should manifest itself in the marked contrast, both in magnitude and in the peak position, between the $\boldsymbol{\sigma}\cdot\mathbf{q}$ and $\boldsymbol{\sigma}\times\mathbf{q}$ nuclear responses.

These ideas are, however, difficult to test since it is not easy to find a probe which couples longitudinally to the nucleonic spins. This indeed occurs only for hadronic (e.g., p,p′) or semihadronic (e.g., e, e′π)[2] probes, which, however, cannot penetrate the nuclear interior owing to their strong absorption. As a consequence, what is actually probed in a hadronic process is the *surface* response of the nucleus rather than the *volume* one. A relevant question is then to ascertain how much of the collective features of a volume response are left out in a surface one.

On the experimental side, two attempts have been made until now to unravel the contrast between the $\boldsymbol{\sigma}\times\mathbf{q}$ and the $\boldsymbol{\sigma}\cdot\mathbf{q}$ channels. In the first one, carried out in Los Alamos,[3] a measurement of the polarization transfer coefficients in the deep inelastic, inclusive, polarized (p,p′) scattering was performed. The ratio $\mathcal{R}$ between R_L and R_T, a critical test of their contrast, can be inferred from these coefficients and was determined as a function of the energy at the fixed momentum transfer $q=1.75$ fm^{-1}. Now, according to the theoretical predictions, $\mathcal{R}$ should largely exceed one; instead, the Los Alamos data pointed to a value of $\mathcal{R}$ close to one and perhaps even smaller. This finding was at first surprising, even for a surface reaction. It should, however, be noticed that a (p,p′) polarized scattering process, while disentangling the $\boldsymbol{\sigma}\cdot\mathbf{q}$ and $\boldsymbol{\sigma}\times\mathbf{q}$ channels, cannot separate, in isospace, the isoscalar and the isovector modes. Hence a careful analysis is required before drawing any conclusion from a (p,p′) experiment.

To avoid this hindrance, recently a charge exchange (He^3,t) experiment, obviously free from the isoscalar contamination, has been carried out at Saturne.[4] Here no polarization transfer variables were measured and the attention was focused on the peak position of the QEP. Indeed the momentum evolution of the latter was followed from 1.4 to 2.4 fm^{-1} and compared with the one observed in deep inelastic (e,e′) scattering. As it is well known, in the latter case the *volume* $\boldsymbol{\sigma}\times\mathbf{q}$ nuclear response is probed.

The relevance of the charge exchange (He^3,t) reaction for the spin-isospin nuclear response relies on the well-established dominance of the isovector ($\tau=1$) spin-flip ($\sigma=1$) nucleon-nucleon (NN) amplitudes over the non-spin-flip ones. However, the former contain both spin-longitudinal and spin-transverse components, in a proportion varying with the momentum. Thus the $\sigma=\tau=1$ nuclear response measured in the highly peripheral (He^3,t) process is in fact a mixture of the $\boldsymbol{\sigma}\times\mathbf{q}$ and $\boldsymbol{\sigma}\cdot\mathbf{q}$ modes. Remarkably in this reaction the maximum of the

QEP was observed to soften progressively, as the momentum increased, with respect to the one of the (e,e') scattering and even with respect to the free Fermi gas prediction. The possibility to ascribe this effect to the increasing weight of R_L in the cross section was then suggested, which appears justified since we know that, as q increases, the $\sigma\cdot\mathbf{q}$ NN amplitude tends to dominate over the $\sigma\times\mathbf{q}$ one. The observed downward shift would then reflect the softening of the spin-longitudinal nuclear response, thus providing a signature for the otherwise elusive role of the pion in nuclear physics.

It should be kept in mind, however, that the (He^3,t) reaction is even more peripheral than the (p,p') one: indeed it explores a nuclear region centered around a quite small value $\bar{\rho}$ of the density, such that $\frac{1}{5}\rho_0 \le \bar{\rho} \le \frac{1}{4}\rho_0$, ρ_0 being the central nuclear density. Whether collective effects can survive at such a low density and, furthermore, up to such large momenta is a challenging question we wish to explore. For this purpose we develop in the present paper a finite nucleus surface response theory, which basically amounts to insert an appropriate vertex function $F(r)$ in the particle-hole RPA polarization propagator. A preliminary version of this approach, with a crude ansatz for $F(r)$, was presented in Ref. 5.

This paper is organized as follows. In Sec. II we outline the derivation of our surface RPA approach, whereas in Sec. III we exploit Glauber theory[6] to determine the vertex function $F(r)$. We then compare the surface and volume free responses in a harmonic oscillator (HO) basis.

In Sec. IV we test our theory against the Los Alamos experiment. The calculation with a realistic vertex function shows how the peripheral nature of the process brings the ratio $\mathcal{R}=R_L/R_T$ down toward unity, partly through the low density experienced by the probe and partly though the mixing of the spin modes. Other groups[7-10] have independently obtained results very similar to ours. However, some discrepancy between theory and experiment is left out, which might signal[11] the existence of some collectivity in the isoscalar spin channel.

In Sec. V we attempt an interpretation of the (He^3,t) data. We show that in spite of the quite peripheral nature of the He^3 probe enough collectivity is left to shift down the maximum of the $\sigma\cdot\mathbf{q}$ response. Relying on the present knowledge of the elementary NN amplitudes we then test our theory against the available data for momenta ranging from 1.4 to 2.4 fm^{-1}. We come to the conclusion that the RPA pion induced correlations, although pointing into the right direction, cannot wholly account for the downward shift experimentally observed. In the same section we also speculate on the possible physical origin of this shortcoming conjecturing, in particular, on the role of relativistic effects to account for it.

II. THE SURFACE RPA FORMALISM

As the strongly interacting probes mainly excite the nuclear surface, one should set up a RPA polarization propagator constrained to have the initial p-h excitation localized in the outer region of the nucleus.

This aim can be achieved for the Jth multipole of the dynamical part $\hat{\Pi}(q,q';\omega)$ of the polarization propagator $\Pi(\mathbf{q},\mathbf{q}';\omega)$ (the geometrical angular factors being dealt with standard methods[12]) through the Dyson equation

$$[\hat{\Pi}_J^{\mathrm{RPA},ss}(q,q';\omega)]_{ll'}=[\hat{\Pi}_J^{0,ss}(q,q';\omega)]_{ll'}+\sum_{l_1 l_2}\int_0^\infty \frac{dk\,k^2}{(2\pi)^3}[\hat{\Pi}_J^{0,s}(q,k;\omega)]_{ll_1}[U_J(k)]_{l_1 l_2}[\hat{\Pi}_J^{\mathrm{RPA},s}(k,q';\omega)]_{l_2 l'}\ , \tag{2.1}$$

where, in turn $[\hat{\Pi}_J^{\mathrm{RPA},s}(q,q';\omega)]_{ll'}$ obeys the following integral equation:

$$[\hat{\Pi}_J^{\mathrm{RPA},s}(q,q';\omega)]_{ll'}=[\hat{\Pi}_J^{0,s}(q,q';\omega)]_{ll'}+\sum_{l_1 l_2}\int_0^\infty \frac{dk\,k^2}{(2\pi)^3}[\hat{\Pi}_J^{0}(q,k;\omega)]_{ll_1}[U_J(k)]_{l_1 l_2}[\hat{\Pi}_J^{\mathrm{RPA},s}(k,q';\omega)]_{l_2 l'}\ . \tag{2.2}$$

Diagrammatically (2.1) and (2.2) are displayed in Fig. 1, where rings with two, one, or no black vertices correspond to $\hat{\Pi}_J^{ss}$, $\hat{\Pi}_J^{s}$, and the volume propagator, respectively. Explicitly, in the independent particle approximation, one has

$$\hat{\Pi}_J^{0,ss}(q,q';\omega)=16\pi\sum_{\substack{n_p l_p\\ n_h l_h}}(2l_p+1)(2l_h+1)\begin{pmatrix} l_p & l_h & J\\ 0 & 0 & 0\end{pmatrix}^2 \mathcal{I}^s_{n_p l_p n_h l_h}(q)\mathcal{D}(\epsilon_p,\epsilon_h;\omega)\mathcal{I}^s_{n_p l_p n_h l_h}(q')\ , \tag{2.3}$$

and

$$\hat{\Pi}_J^{0,s}(q,q';\omega)=16\pi\sum_{\substack{n_p l_p\\ n_h l_h}}(2l_p+1)(2l_h+1)\begin{pmatrix} l_p & l_h & J\\ 0 & 0 & 0\end{pmatrix}^2 \mathcal{I}_{n_p l_p n_h l_h}(q)\mathcal{D}(\epsilon_p,\epsilon_h;\omega)\mathcal{I}^s_{n_p l_p n_h l_h}(q')\ , \tag{2.4}$$

with

$$\mathcal{D}(\epsilon_p,\epsilon_h;\omega)=\frac{1}{\hbar\omega-(\epsilon_{n_p l_p}-\epsilon_{n_h l_h})+i\eta}-\frac{1}{\hbar\omega+(\epsilon_{n_p l_p}-\epsilon_{n_h l_h})-i\eta}\ , \tag{2.5}$$

$$\mathcal{I}^s_{l n_p l_p n_h l_h}(q)=q\int_0^\infty dr\,r^2 j_l(qr)R_{n_p l_p}(r)R_{n_h l_h}(r)F(r)\ , \tag{2.6}$$

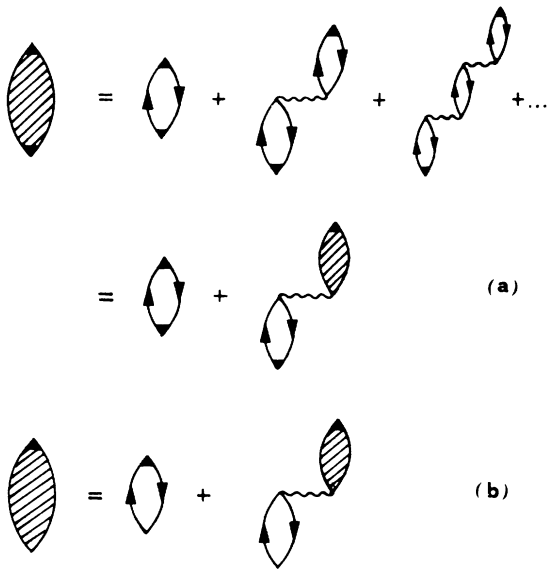

FIG. 1. Diagrams embodied in Eqs. (2.1) (a) and (2.2) (b): the black vertices contain the vertex function (2.7); the p-h propagator includes both N-h and Δ-h excitations.

and in the $\mathcal{J}_{ln_p l_p n_h l_h}$ without the superscript s the function $F(r)$, to be later discussed, is replaced by one; the definition of $\hat{\Pi}^0_l$ is then obvious. It should be noticed that the free $\hat{\Pi}^0_l$'s are diagonal in the angular momentum indices only when the spin-orbit term in the nuclear mean field is neglected (an assumption we shall make in the following, for simplicity); for the single particle energies ϵ_{nl} and the radial wave function R_{nl} we choose an HO basis.

Concerning the quantity $F(r)$, it should be observed that the present approach, at variance with the volume RPA theory,[13] introduces a new excitation operator according to the the following replacement:

$$e^{i\mathbf{q}\cdot\mathbf{r}} \Longrightarrow F(r)e^{i\mathbf{q}\cdot\mathbf{r}} , \tag{2.7}$$

$\mathbf{r}$ being the distance from the center of the nucleus. Thus $F(r)$ assumes the significance of a vertex function, accounting for the distortion of the hadronic field as it approaches the nucleus.

How to determine $F(r)$ will be discussed in the next section. Here we point out that the presence of the vertex function does not necessarily confine the excitations engrained in $\hat{\Pi}^{\mathrm{RPA},ss}$ on the nuclear surface; it only compels them to "originate" there: afterwards they can propagate everywhere inside the nucleus. Whether they actually will do that depends on the nature of the p-h interaction. For the latter we use the $\pi+\rho$-exchange potential, customarily used in the spin-isospin channel. The standard expression of the required partial waves reads

$$[U_J(k)]_{ll'} = a_{Jl}a_{Jl'}V_L(k) + (\delta_{ll'} - a_{Jl}a_{Jl'})V_T(k) , \tag{2.8}$$

being

$$a_{Jl} = (-1)^l\sqrt{2l+1}\begin{bmatrix} l & 1 & J \\ 0 & 0 & 0 \end{bmatrix} , \tag{2.9}$$

and

$$V_L(k) = \Gamma_\pi^2(k^2)\frac{f_\pi^2}{\mu_\pi^2}\left[g' - \frac{k^2}{k^2+\mu_\pi^2}\right]\frac{1}{k^2} , \tag{2.10}$$

$$V_T(k) = \left[\Gamma_\pi^2(k^2)\frac{f_\pi^2}{\mu_\pi^2}g' - \Gamma_\rho^2(k^2)\frac{f_\rho^2}{\mu_\rho^2}\frac{k^2}{k^2+\mu_\rho^2}\right]\frac{1}{k^2} . \tag{2.11}$$

In the above, $f_\pi^2/4\pi\hbar c = 0.08$, $f_\rho^2/\mu_\rho^2 = 2.18 f_\pi^2/\mu_\pi^2$, and the usual monopole form factors are included at the $\pi(\rho)$NN vertices [with $\Lambda_\pi(\Lambda_\rho) = 1.3$ (1.7) GeV, respectively]. The short-range repulsive p-h force is embodied in the Landau-Migdal parameter g', taken as constant.

In the actual calculations we also include the Δ resonance, bound, for sake of simplicity, by the same HO mean field felt by the nucleons. Moreover, we assume universality of the NN, NΔ, and ΔΔ interactions (obviously with a different πNΔ vertex). Note that, although not explicitly indicated, the frequency dependence of the interaction has always been taken into account.

We should now solve Eqs. (2.1) and (2.2). To lighten the heavy numeric associated with this task we resort, as in our previous work,[13,5] to the approximation method originally proposed by Toky and Weise.[14] For this purpose we consider the first iteration of (2.2).

$$[\hat{\Pi}^{(1),s}_J(\mathbf{q},\mathbf{q}';\omega)]_{ll'} = \int_0^\infty \frac{dk\,k^2}{(2\pi)^3}\hat{\Pi}^0_l(\mathbf{q},k;\omega) \times [U_J(k)]_{ll'}\hat{\Pi}^{0,s}_{l'}(k,\mathbf{q}';\omega) , \tag{2.12}$$

and fix an average momentum p such that

$$[\hat{\Pi}^{(1),s}_J(\mathbf{q},\mathbf{q}';\omega)]_{ll'} = \frac{\gamma p^2}{(2\pi)^3}\hat{\Pi}^{0,s}_l(\mathbf{q},\mathbf{q}';\omega) \times [U_J(p)]_{ll'}\hat{\Pi}^0_{l'}(p,p;\omega) , \tag{2.13}$$

where the parameter $\gamma \simeq \pi/R$ (R being the rms radius of the nucleus) gives the right dimensions to the right-hand side (rhs) of (2.13). With the help of (2.13) it is then possible to show that the system of integral equations (2.2) reduces to the following system of algebraic equations:

$$[\hat{\Pi}^{\mathrm{RPA},s}_J(\mathbf{q},\mathbf{q}';\omega)]_{ll'} = \delta_{ll'}\hat{\Pi}^{0,s}_l(\mathbf{q},\mathbf{q}';\omega) + \sum_{l_1}[\hat{\Pi}^{\mathrm{RPA},s}_J(\mathbf{q},\mathbf{q}';\omega)]_{ll_1}[\tilde{U}_J(p)]_{l_1l'}\hat{\Pi}^0_{l'}(p,p;\omega) , \tag{2.14}$$

having set

$$[\tilde{U}_J(p)]_{ll'} = \frac{\gamma p^2}{(2\pi)^3}[U_J(p)]_{ll'} . \tag{2.15}$$

The solutions of (2.14) can be inserted into (2.1) to get the angular momentum matrix elements of the various multipoles J of the surface polarization propagator. As an example we quote here one of the five matrix elements needed, for fixed J, to get the expressions of the $\sigma\tau$ nuclear responses, namely

$$[\hat{\Pi}_J^{\mathrm{RPA},ss}(q,q';\omega)]_{J+1,J+1}=\hat{\Pi}_{J+1}^{0,ss}(q,q';\omega)+\frac{1}{D_J(p,\omega)}\{[\hat{\Pi}_J^{(1),ss}(q,q';\omega)]_{J+1,J+1}[1-[\tilde{U}_J(p)]_{J-1,J-1}\hat{\Pi}_{J-1}^{0}(p,p;\omega)]+[\hat{\Pi}_J^{(1),ss}(q,q';\omega)]_{J+1,J-1}[\tilde{U}_J(p)]_{J-1,J+1}\hat{\Pi}_{J+1}^{0}(p,p;\omega)\}\ , \tag{2.16}$$

where

$$D_J(p,\omega)=1-[\tilde{U}_J(p)]_{J-1,J-1}\hat{\Pi}_{J-1}^{0}(p,p;\omega)-[\tilde{U}_J(p)]_{J+1,J+1}\hat{\Pi}_{J+1}^{0}(p,p;\omega)+\tilde{V}_L(p)\tilde{V}_T(p)\hat{\Pi}_{J-1}^{0}(p,p;\omega)\hat{\Pi}_{J+1}^{0}(p,p;\omega)\ . \tag{2.17}$$

When (2.17) (and the like) are inserted (with $q=q'$) into the appropriate combinations of multipolarities,[13] one finally gets

$$R_L^{\mathrm{surf}}(q,\omega)=R_L^{0,\mathrm{surf}}(q,\omega)-\frac{1}{8\pi^2}\mathrm{Im}\sum_{J=0}^{\infty}\left\{\frac{J[\hat{\Pi}_J^{(1),ss}(q,\omega)]_{J-1,J-1}-\sqrt{J(J+1)}[\hat{\Pi}_J^{(1),ss}(q,\omega)]_{J+1,J-1}}{1-\tilde{V}_L(p)\hat{\Pi}_{J-1}^{0}(p,\omega)+(J+1)\mathcal{G}_{J+1}(p,\omega)/(2J+1)}+\frac{(J+1)[\hat{\Pi}_J^{(1),ss}(q,\omega)]_{J+1,J+1}-\sqrt{J(J+1)}[\hat{\Pi}_J^{(1),ss}(q,\omega)]_{J-1,J+1}}{1-\tilde{V}_L(p)\hat{\Pi}_{J+1}^{0}(p,\omega)+J\mathcal{G}_{J-1}(p,\omega)/(2J+1)}\right\}, \tag{2.18}$$

and

$$R_T^{\mathrm{surf}}(q,\omega)=R_T^{0,\mathrm{surf}}(q,\omega)-\frac{1}{16\pi^2}\mathrm{Im}\sum_{J=0}^{\infty}\left\{(2J+1)\frac{[\hat{\Pi}_J^{(1),ss}(q,\omega)]_{J,J}}{1-\tilde{V}_T(p)\hat{\Pi}_J^{0}(p,\omega)}+\frac{(J+1)[\hat{\Pi}_J^{(1),ss}(q,\omega)]_{J-1,J-1}+\sqrt{J(J+1)}[\hat{\Pi}_J^{(1),ss}(q,\omega)]_{J+1,J-1}}{1-\tilde{V}_T(p)\hat{\Pi}_{J-1}^{0}(p,\omega)+J\mathcal{F}_{J+1}(p,\omega)/(2J+1)}+\frac{J[\hat{\Pi}_J^{(1),ss}(q,\omega)]_{J+1,J+1}+\sqrt{J(J+1)}[\hat{\Pi}_J^{(1),ss}(q,\omega)]_{J-1,J+1}}{1-\tilde{V}_T(p)\hat{\Pi}_{J+1}^{0}(p,\omega)+(J+1)\mathcal{F}_{J-1}(p,\omega)/(2J+1)}\right\}, \tag{2.19}$$

which display their collective behavior in a term added to the free response. In the above

$$\mathcal{F}_{J-1}(p,\omega)=[\tilde{V}_T(p)-\tilde{V}_L(p)]\frac{\hat{\Pi}_{J+1}^{0}(p,\omega)-\hat{\Pi}_{J-1}^{0}(p,\omega)}{1-\tilde{V}_L(p)\hat{\Pi}_{J-1}^{0}(p,\omega)}=\mathcal{G}_{J-1}[p,\omega,\tilde{V}_L\rightleftharpoons\tilde{V}_T]\ , \tag{2.20}$$

and

$$\mathcal{F}_{J+1}(p,\omega)=[\tilde{V}_T(p)-\tilde{V}_L(p)]\frac{\hat{\Pi}_{J-1}^{0}(p,\omega)-\hat{\Pi}_{J+1}^{0}(p,\omega)}{1-\tilde{V}_L(p)\hat{\Pi}_{J+1}^{0}(p,\omega)}=\mathcal{G}_{J+1}[p,\omega,\tilde{V}_L\rightleftharpoons\tilde{V}_T]\ . \tag{2.21}$$

Note that, like in the volume responses, no internal surface vertex enters into the ring series of (2.18) and (2.19). One should also notice that these reduce to the corresponding $\sigma\tau$ volume responses [see formulae (3.3) and (3.6) of Ref. 13] when all the surface vertices are replaced by the volume ones with the $\hat{\Pi}_J^{(1)}$'s explicitly appearing in (2.18) and (2.19) expressed by means of formula (2.13).

The above surface spin-longitudinal and spin-transverse nuclear responses require the evaluation, for any given q, ω, and J, of two exact first-order polarization propagators, one *surface to volume* [cf. (2.12)] to settle the value of p and one *surface to surface* which directly enters into their expressions: as a consequence the numerical computation of $R_L^{\mathrm{surf}}(R_T^{\mathrm{surf}})$ is heavier than for $R_L^{\mathrm{vol}}(R_T^{\mathrm{vol}})$.

Like in the latter, the functions $\mathcal{F}$ and $\mathcal{G}$ in the surface responses explicitly account for the mixing between the two spin modes and for further effects associated with the lowering of the density in going from the central to the outer region of the nucleus. These finite system features, partly embodied also in the average momentum p, work more efficiently against collectivity in the surface than in the volume response. In this connection we notice that $\mathcal{F}$ and $\mathcal{G}$ are proportional to the difference of the two forces, $V_L(p)-V_T(p)$. Since in general p turns out, numerically,

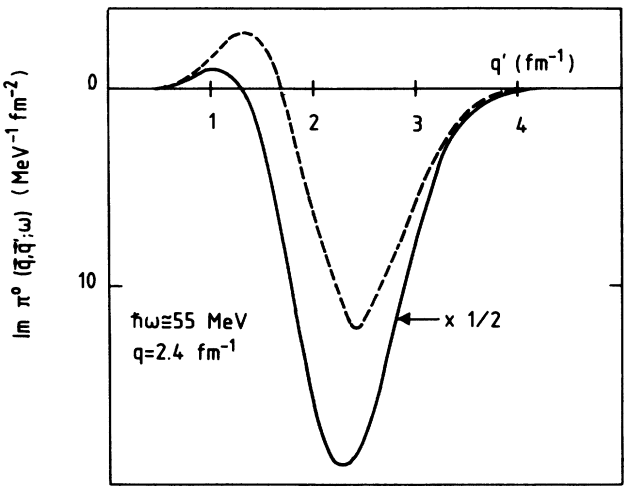

FIG. 2. The imaginary part of $\Pi^0(\mathbf{q},\mathbf{q}';\omega)$ (Ref. 12) (solid line) and $\Pi^{0,s}(\mathbf{q},\mathbf{q}';\omega)$ (dashed line) at fixed $q=2.4$ fm^{-1}, $\hbar\omega\cong 55$ MeV, and $\hat{\mathbf{q}}\cdot\hat{\mathbf{q}}'=1$, as a function of q', for Ca^{40}.

to be rather close to q, $\mathcal{F}$ and $\mathcal{G}$ are large precisely where one would expect to have the largest contrast between the spin-isospin responses. Accordingly the momentum evolution of the latter should result somewhat tempered.

Concerning the validity of the approximation scheme utilized in solving the RPA equations, we expect it to be fairly accurate when the nonlocality in the momentum space of the HO polarization propagators $\hat{\Pi}^0_J$ and $\hat{\Pi}^{0,s}_J$ is moderate. To illustrate this point we display in Fig. 2 the behavior of the imaginary part of the volume and surface free polarization propagators $\Pi^0(\mathbf{q},\mathbf{q}';\omega)$ and $\Pi^{0,s}(\mathbf{q},\mathbf{q}';\omega)$, for fixed q and ω, as a function of q' in Ca^{40}. One can see that although the "bell" representing $\mathrm{Im}\Pi^0$ is indeed narrower than the one corresponding to $\mathrm{Im}\Pi^{0,s}$, still both of them are markedly peaked in momentum space. However, whereas the volume propagator considerably shrinks in going to heavier nuclei, as shown in Ref. 13, the surface one is substantially independent of the mass number A.

We can then expect the Toki and Weise method to provide a reliable approximation for the nuclear response functions, but, of course, its final test can only come from large scale, accurate RPA calculations with finite range forces.

III. THE VERTEX FUNCTION $F(r)$

Although RPA calculations in finite nuclei on a large Hilbert basis are not yet available, still the semi-infinite slab model (SIS) of Esbensen and Bertsch.[15] has been of great importance in providing us with new insights into the surface response functions. We shall follow here their approach, which is based on Glauber's theory of nuclear reactions[16] to evaluate the vertex function $F(r)$.

To start with, the basic assumption is to view the reaction as a single scattering process. Double scattering, much harder to calculate, should eventually contribute to the experimentally detected background and to the responses at larger energies. Under these circumstances the number of nucleons effectively responding to the external probing field can be expressed as follows:

$$N_{\mathrm{eff}}=\frac{\sigma^{(1)}}{\sigma_{\mathrm{tot}}}\ , \tag{3.1}$$

where the single-step reaction cross-section reads

$$\sigma^{(1)}=2\pi\int_0^\infty db\, b\chi(b)e^{-\chi(b)}\ , \tag{3.2}$$

the phase shift function (responsible for the attenuation of the incoming wave) being

$$\chi(b)=\sigma_{\mathrm{tot}}\int_{-\infty}^{+\infty}dz\,\rho[r=(b^2+z^2)^{1/2}]\ . \tag{3.3}$$

In the above formulae ρ is the nuclear density and σ_{tot} the total probe-nucleon cross section at the considered energy.

Now the same quantity N_{eff} can as well be determined through sum rule arguments. Indeed, for momenta large enough to neglect the restrictions due to the Pauli principle, one has, for a spherical nucleus[15]

$$N_{\mathrm{eff}}=\int_0^\infty d\omega\, R(\mathrm{q},\omega)=4\pi\int_0^\infty dr\, r^2\,|F(r)|^2\rho(r)\ , \tag{3.4}$$

where $R(\mathrm{q},\omega)$ is the nuclear response to the driving field in the rhs of (2.7). Hence, by comparing with (3.1), it follows

$$4\pi r^2\,|F(r)|^2\rho(r)=\frac{2\pi}{\sigma_{\mathrm{tot}}}r\chi(r)e^{-\chi(r)}\ , \tag{3.5}$$

which fixes $F(r)$. The above procedure is strictly valid in the SIS model, where the same cylindrical geometry of the eikonal description holds good; in our framework, where the geometry is spherical, it remains substantially valid.

Formula (3.5) allows us to explore how deeply the impinging field probes the target nucleus. This, as well as the magnitude of the reaction cross sections (He^3,t) or (p,p') crucially depends upon the value of the total cross section σ_{tot} for the probe-nucleon interaction [see Eq. (5.1)]. In the case of the proton probe this cross section is $\sigma_{\mathrm{tot}}=40$ mb at the incident energy of 500 MeV. In the case of the He^3 probe one would expect three times the nucleon value, i.e., $\cong 120$ mb.

However, according to the analysis performed by Gaarde,[17] this value inserted in (3.1) and (5.1) would yield a magnitude for the (He^3,t) reaction cross section smaller than the experimental value by almost a factor 2. Instead the value required to get agreement with the data is $\sigma_{\mathrm{tot}}=55$ mb. As a comment about this large difference one should realize that the present treatment avoids a microscopic description of the He^3 interaction with the bound nucleons. It is possible, for instance, that the difference between the two cross sections, if it does not arise from mechanisms beyond the one-step process, reflects the finite range of the He^3-N interaction, which is ignored in the present treatment.

We have adopted in our analysis of the (He^3,t) reaction the value $\sigma_{\mathrm{tot}}=55$ mb, but we have as well explored the situation corresponding to $\sigma_{\mathrm{tot}}\cong 105$ mb. We then display in Fig. 3 the function $S(r)=r^2\,|F(r)|^2\rho(r)$ in ar-

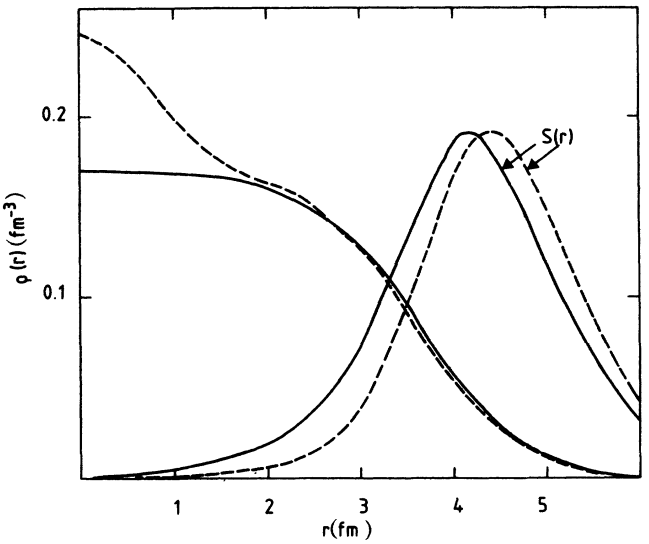

FIG. 3. Empirical (solid line) and HO (dashed line) densities in Ca^{40}; the HO parameter is $\hbar\omega_0 = 11.02$ MeV. The function $S(r)$ (see text) is also drawn, with an arbitrary scale, for $\sigma_{tot} = 40$ mb (solid line) and $\sigma_{tot} = 55$ mb (dashed line).

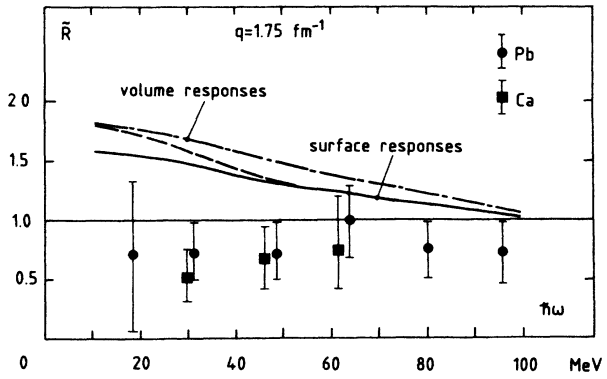

FIG. 4. The ratio $\tilde{\mathcal{R}}$ (4.1) at $q = 1.75$ fm^{-1} as a function of ω. The experimental points are taken from Ref. 2; the dot-dashed line is the prediction of our RPA theory of the *volume* responses; the *surface* RPA prediction for $\tilde{\mathcal{R}}$ is given by the solid and the dashed lines, with and without mixing of the spin modes, respectively; $g' = 0.7$. The isoscalar responses are assumed to be the free ones.

bitrary units, together with the experimental and HO densities (almost identical in the surface region) for Ca^{40}. As expected, one sees that the smaller σ_{tot} is, the more the probing field penetrates inside the nucleus. Numerically, for $\sigma_{tot} = 40$ mb, the peak of $S(r)$ corresponds to a density $\bar{\rho} \cong 0.28\rho_0$ (ρ_0 being the central nuclear density), whereas, for $\sigma_{tot} = 55$ mb, the peak moves outward to a region where $\bar{\rho} \cong 0.20\rho$.

The central question is then to ascertain if in such dilute media the p-h interaction is still capable to set up collective effects. In this connection it is worth realizing that the number of nucleons effectively taking part in the processes turns out to be, from (3.4), $N_{eff} = 5.3$ and 3.6 for the two cases.

IV. THE RATIO BETWEEN THE ISOVECTOR SPIN-NUCLEAR RESPONSES

Carey *et al.*[3] measured the spin observables in the deep inelastic scattering of 500 MeV polarized protons out of Ca^{40} and Pb.[208] The experiment focused on the energy behavior of the ratio R_L/R_T. This quantity indeed should be sensitive to the simultaneous enhancement of R_L and quenching of R_T, particularly at the chosen value of the momentum, $q = 1.75$ fm^{-1}, where the contrast is expected to be strong.

However, this experiment cannot separate the isovector contribution ($\tau = 1$) from the isoscalar one ($\tau = 0$). Consequently, it measures, in fact, the combination

$$\tilde{\mathcal{R}} = \frac{2.15}{4.62} \frac{3.62R_L^{\tau=1}(q,\omega) + R_L^{\tau=0}(q,\omega)}{1.15R_T^{\tau=1}(q,\omega) + R_T^{\tau=0}(q,\omega)} , \tag{4.1}$$

which, in spite of the substantial isoscalar contamination, was expected to still show some vestiges of collectivity.

In Fig. 4 we show, as a function of the excitation energy, $\tilde{\mathcal{R}}$ calculated from our isovector RPA surface responses, R_L^{surf} and R_T^{surf}, with $g' = 0.7$ and taking for the isoscalar response the free ones. The vertex function $F(r)$ is evaluated from Eq. (3.5) with $\sigma_{tot} = 40$ mb. Both the curves with and without the mixing between the spin modes are displayed, together with the quantity $\tilde{\mathcal{R}}$ obtained from the volume responses.

The role of the nuclear surface in bringing $\tilde{\mathcal{R}}$ down towards unity, particularly at low frequencies, can be appreciated, a finding supported by quite similar results obtained by other authors.[7–10] The nuclear surface hampers collective effects partly because of its low, rapid-

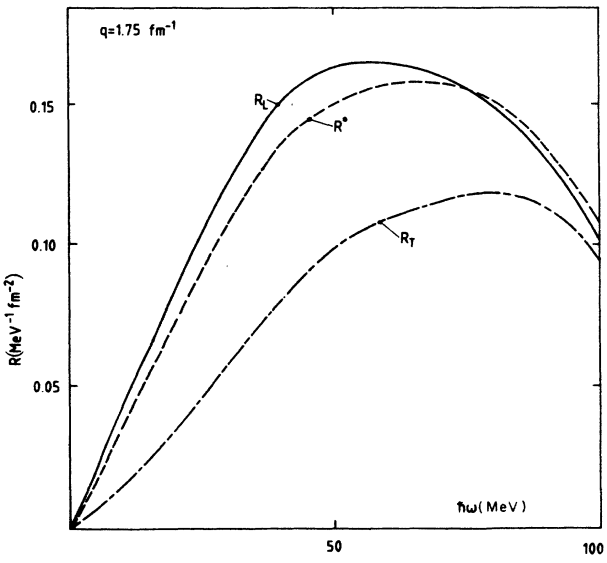

FIG. 5. Surface free (dashed line), surface RPA spin-longitudinal (solid line), and spin-transverse (dot-dashed line) isovector responses in Ca^{40} at $q = 1.75$ fm^{-1}, as a function of ω, for $g' = 0.7$. The vertex function $F(r)$ corresponds to the solid curve in Fig. 3.

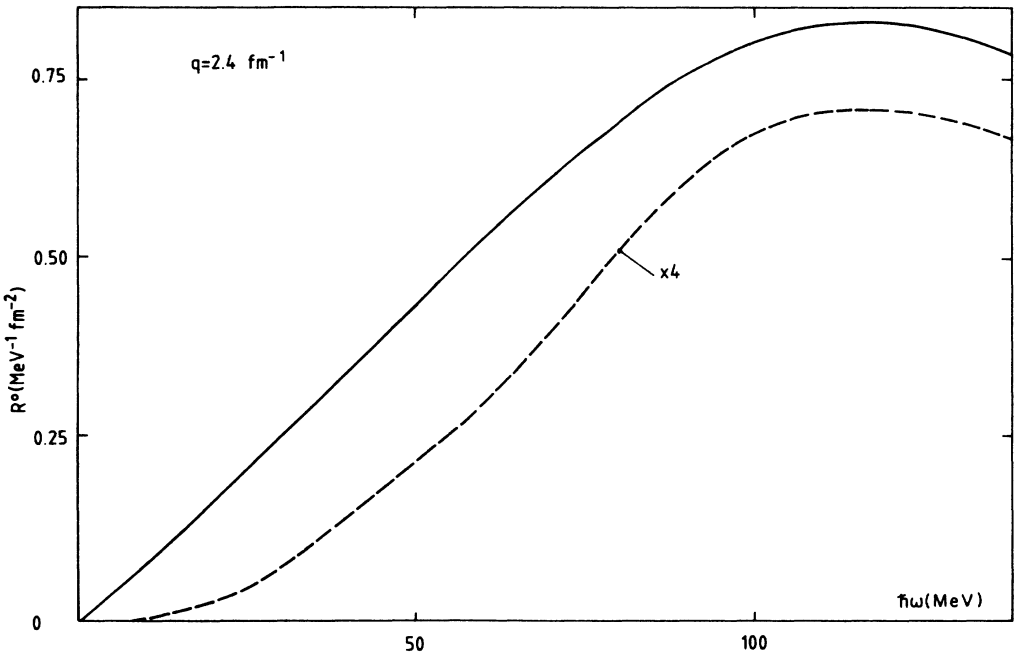

FIG. 6. Independent particle *volume* (solid line) and *surface* (dashed line) responses at $q=2.4$ fm^{-1}, as a function of ω, in Ca^{40}; the vertex function $F(r)$ in the surface response corresponds to the dashed curve in Fig. 3.

ly varying density and partly because it couples the $\sigma\cdot\mathbf{q}$ and $\sigma\times\mathbf{q}$ modes. In connection with this last point one should notice that the A-independent mixing is significantly effective *only* at low frequencies and for those momenta where the force mixed in the opposite channel is substantial, which is the case, at $q=1.75$ fm^{-1}, for the mixing of the transverse interaction into R_L.

Yet some discrepancy between theory and experiment is left out and could be significantly reduced utilizing a value for g' larger than 0.7. This would, however, bring us in conflict with the inclusive (e,e') data[13] and also with those of the (He^3,t) reaction to be discussed later on.

As an alternative explanation, it has been argued[11] that the nuclear responses in the $\sigma=1$, $\tau=0$ channel should not be described in a mean field framework, but rather in a RPA one. Indeed in this channel some collective behavior is also expected and, characteristically, of a nature just opposite to the one affecting the $\tau=1$ spin modes; hence, a further reduction of $\tilde{\mathcal{R}}$ would follow.

In concluding this section we show in Fig. 5 separately our isovector R_L^{surf} and R_T^{surf} in Ca^{40}, with $F(r)$ corresponding to $\sigma_{\text{tot}}=40$ mb, at $q=1.75$ fm^{-1}. By comparing them with the free *surface* response, also displayed, we can appreciate the persistence of a substantial amount of collectivity, particularly in the transverse channel, in spite of the low density experienced by the probe and the large momentum transfer.

To shed further light on the surface role, in Fig. 6 we compare the independent particle volume and surface responses. We see that the surface, through the vertex function $F(r)$, much reduces the magnitude of the response, but leaves almost unaltered its shape.

V. THE NUCLEAR SPIN-LONGITUDINAL ISOVECTOR RESPONSE

The discussion in the previous section reminded the necessity of probing the nucleus with pure isovector processes in order to gain a real insight into the pion role in nuclear structure. This was realized with the high-energy *isovector* charge-exchange (He^3,t) reaction carried out at Saturne by Bergqvist *et al.*[4]

This experiment stressed the remarkable feature of the nuclear spin-isospin collective phenomena to survive under conditions of quite low density and short wavelengths. Indeed, Bergqvist *et al.* were able to detect a downward shift of the peak position ω_M of the QEP with respect to the corresponding peak of the free Fermi gas. Since He^3, at the bombarding energy of 2 GeV, is a good spin-isospin probe, it would seem that these authors were in fact able to unravel the elusive softening of the spin-longitudinal isovector response. Whether their experiment involves the *pure* $\sigma\cdot\mathbf{q}$ response is a question to be addressed: we shall return later on this difficulty.

In Fig. 7 we display, in C^{12}, the maxima of the experimental cross sections. Also shown are the corresponding quantities for a nonrelativistic ($\omega_M=q^2/2M$) and a relativistic ($\omega_M=q_\mu^2/2M$) Fermi gas, the latter being appreciably lower than the former at large q.

In Ref. 4 Bergqvist *et al.* point out that spectra of C^{12} and Ca^{40} practically overlap each other, but for a normalization factor which is the same at all scattering angles. This finding is a clear signature of the surface character of the process. Accordingly, in Fig. 7, the experimental points of C^{12} can be attributed as well to Ca^{40}. In the

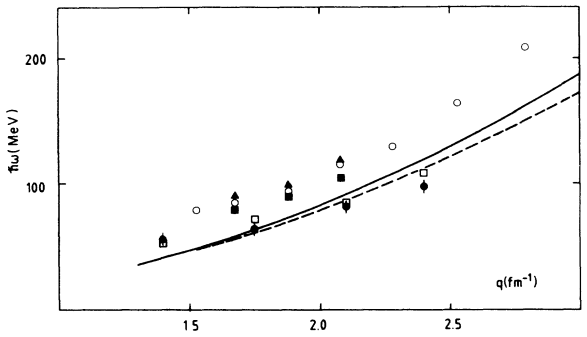

FIG. 7. Peak position for the QEP in the reactions C^{12} (He^3,t) at 2 GeV (Ref. 4) (dots) and Ca^{40}(e,e') (Ref. 18) (circles); theoretical predictions from Ref. 13 for the volume p-h RPA (black squares) and the p-h RPA + 2p-2h (triangles) isovector transverse responses are also displayed; the open squares are the surface RPA predictions for the (He^3,t) reaction; solid and dashed lines represent the peak positions of the nonrelativistic and relativistic Fermi gas responses, respectively.

same figure we also display the experimental maxima of the *separated* transverse response taken from (e,e') scattering[18] (in Ref. 4, instead, the maxima of the *global* response of C^{12} were reported). A substantial hardening with respect to the free Fermi gas is seen to occur, which we ascribe[13] partly to the RPA correlations induced by the repulsive transverse interaction V_T and partly to the 2p-2h excitations, whose contribution to the volume nuclear responses is substantial.

The real challenge of Fig. 7 lies in the (He^3,t) results and the question to be asked is whether the theory can explain the observed softening at a momentum transfer as large as 2.4 fm^{-1}, given the highly peripheral nature of the (He^3,t) reaction. With $\sigma_{tot}=55$ mb the vertex function $F(r)$, displayed in Fig. 3, peaks at the low density of $0.20\rho_0$.

With this $F(r)$ we have calculated the surface spin-longitudinal RPA response (with $g'=0.7$) and the free one at $q=2.4$ fm^{-1}, i.e., where an impressive downward shift of about 18 MeV, with respect to the nonrelativistic Fermi gas, is being exhibited by the data. Our results are displayed in Fig. 8: the surface RPA curve is weakly enhanced and softened by about 8 MeV with respect to the free one. This amount is less than required by the experiment, but still significant, signalling that the pion induced correlations are not entirely washed out at these low densities. A reduction of the short-range repulsion in the p-h interaction would increase the collectivity. For example, with $g'=0.6$, the shift becomes of 11 MeV, but, at the same time, the disagreement with the Los Alamos data for the ratio $\tilde{R}$ (4.1) worsens. This could be not that serious, however, since the isoscalar spin contribution might be so substantial to compensate for it.[11]

We turn now to assess quantitatively the validity of our theory on the (He^3,t) experiment. This requires a control of the NN charge-exchange amplitudes, since the spin-longitudinal and the spin-transverse responses are mixed in the process. According to Refs. 4 and 19, at the energy of 667 MeV the non-spin-transfer NN charge-

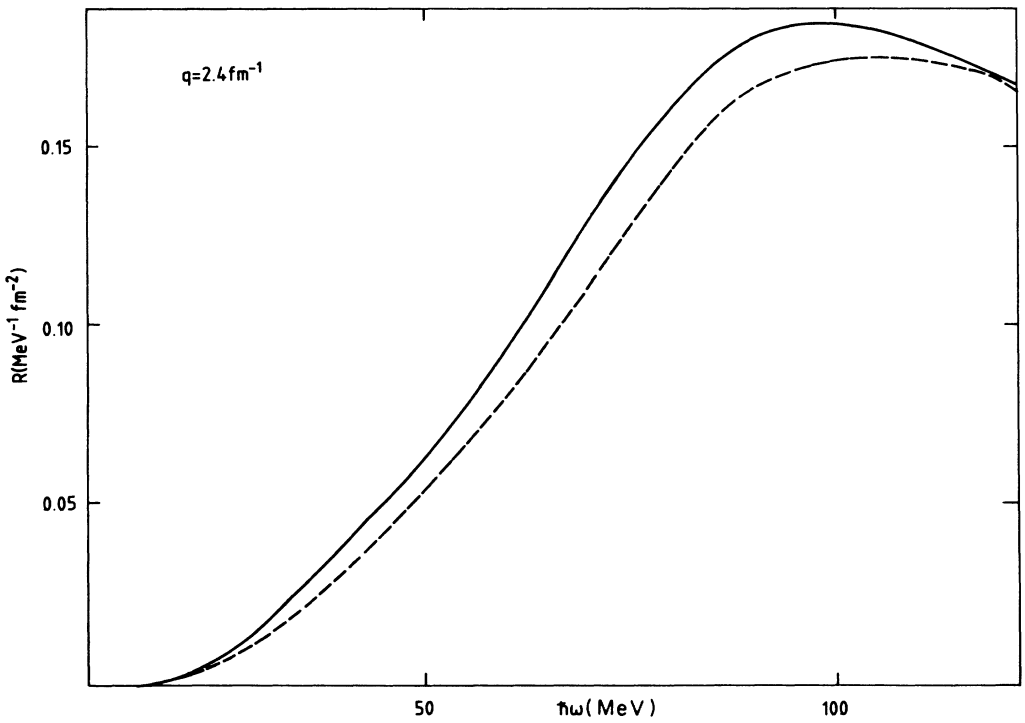

FIG. 8. Surface spin-longitudinal RPA (solid line) and surface free (dashed line) isovector responses at $q=2.4$ fm^{-1} as a function of ω, in Ca^{40}, for the (He^3,t) reaction; $g'=0.7$.

exchange amplitudes, as well as the spin-orbit one, are negligible and the (He^3,t) reaction cross section can be written as follows:

$$\frac{d^2\sigma}{d\Omega\, d\omega} = N_{\text{eff}}[(|\beta|^2 + |\epsilon|^2)R_T(q,\omega) + |\delta|^2 R_L(q,\omega)]FF^2 , \quad (5.1)$$

FF being the (He^3,t) form factor, β and ϵ the charge-exchange spin-transverse NN amplitudes, and δ the spin-longitudinal one, in the notation of Ref. 20. Thus (5.1) is a *combination* of the spin-transverse and spin-longitudinal isovector nuclear responses in a proportion varying with q.

However, the ratio $|\delta|^2/|\beta|^2 + |\epsilon|^2$ is almost

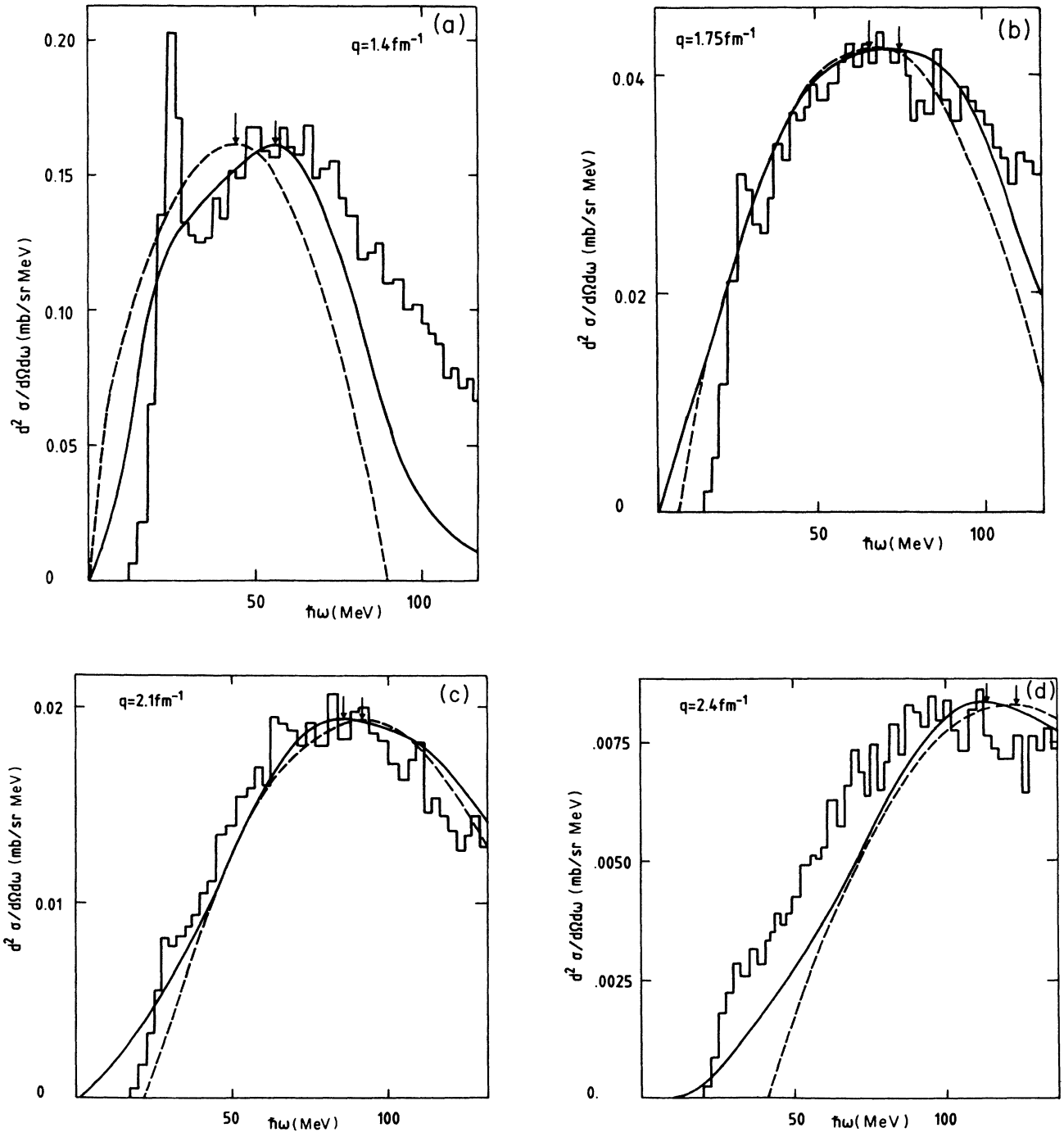

FIG. 9. (a) Experimental and surface RPA (solid line) cross sections for the (He^3,t) reaction at $q = 1.4$ fm^{-1}, as a function of ω; $g' = 0.6$. The cross section for a nonrelativistic Fermi gas is also shown for comparison, with $k_F = 0.79$ fm^{-1}. Arrows indicate the peak position. (b) As in (a), at $q = 1.75$ fm^{-1}. (c) As in (a), at $q = 2.1$ fm^{-1}. (d) As in (a), at $q = 2.4$ fm^{-1}.

linearly increasing from 0.4 at $q=1.4$ fm^{-1} up to 1.5 at $q=2.4$ fm^{-1} (Refs. 4 and 30); therefore, in practice, at large q, the $\sigma\cdot\mathbf{q}$ amplitude dominates the cross section.

Since our approximation scheme in solving the RPA equations works better in a medium size nucleus, we have calculated the cross section (5.1) in Ca^{40} utilizing the NN amplitudes of Ref. 19 to suitably combine our surface RPA responses. Note that the (He^3,t) form factor *FF* is not evaluated, but it is included in the arbitrary normalization factor, the same for all the four cases we have analyzed. Furthermore, we have taken $g'=0.6$, which better accounts for the data. Our results are displayed in Figs. 9(a)–9(d) together with the experimental data and the free nonrelativistic Fermi gas cross section (at the density of $0.20\rho_0$). The RPA cross section is seen to be hardened with respect to the Fermi gas at $q=1.4$ fm^{-1}, where the $\sigma\times\mathbf{q}$ channel is preponderant, in accord with the data. At larger momenta ($q=2.4$ fm^{-1}) the $\sigma\cdot\mathbf{q}$ channel dominates and the RPA cross section is softened by 10 MeV, in qualitative, but not quantitative, accord with the experiment. It is noteworthy that at this momentum the influence of R_T is barely felt (10 MeV of softening versus 11 MeV for a pure $\sigma\cdot\mathbf{q}$ coupling).

A noticeable feature of the data is the substantial tail of the cross section on the high energy side. This tail is present as well in the (e,e') data, where it arises from 2p-2h excitations. It is surprising that this contribution remains so prominent in a process involving the low density nuclear surface.

Concerning the failure of our theory to quantitatively account for the softening of the peak in the (He^3,t) cross section at large q, the use of relativistic kinematics[21] would help in this connection. In fact, at $q=2.4$ fm^{-1}, the free relativistic response is softened by 6.8 MeV with respect to the nonrelativistic one (but only by 2 MeV at $q=1.75$ fm^{-1}). If combined with the RPA softening, this would almost completely account for the experiment.

As for the value of g' employed ($g'=0.6$), it appears somewhat lower than the usually accepted values. However, in our approach, we rely on the assumption of universality ($g'_{NN}=g'_{N\Delta}=g'_{\Delta\Delta}$), which is too crude. Our softening could in fact reflect the action of the Δ, which is likely to experience a weaker short-range repulsion ($g'_{N\Delta}<g'_{NN}$). In addition, according to a recent analysis,[22] the low density of the nuclear surface would also help in reducing the value of g'.

Thus it appears that the momentum evolution of the quasi-elastic peak is satisfactorily reproduced in the RPA framework for the nuclear responses, with acceptable values for the Landau-Migdal parameter and the inclusion of some relativistic corrections. However, we stress that this has been achieved with the value $\sigma_{\rm tot}=55$ mb for the He^3-nucleon cross section. If we use instead three times the value of the nucleon-nucleon cross section (105 mb), the reaction becomes even more peripheral, reducing the RPA shifts. Indeed, at $q=2.4$ fm^{-1} we find that the RPA softening is practically washed out, the shift in the cross section being reduced to about 3 MeV.

In concluding this section we shortly comment on the origin of the collectivity in the $\sigma\cdot\mathbf{q}$ channel at such a low density and short wavelengths. For this purpose, it helps

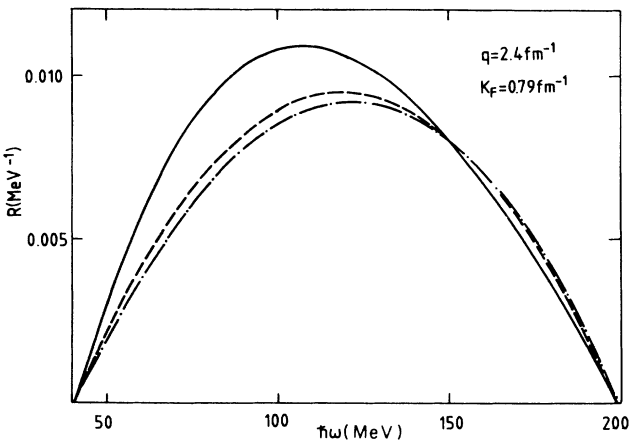

FIG. 10. Nuclear matter free (dashed line), RPA spin-longitudinal (solid line) and RPA spin-transverse (dot-dashed line) isovector responses at $q=2.4$ fm^{-1}, for $g'=0.6$; $k_F=0.79$ fm^{-1}.

to consider nuclear matter at low density, say $0.2\rho_0$, the one explored with $\sigma_{\rm tot}=55$ mb, and compare the corresponding responses R_L^{nm} and R_T^{nm} at $q=2.4$ fm^{-1}. This we have done in Fig. 10, where it appears that while some vestiges of collectivity are still present in R_L^{nm}, practically nothing of it is left in R_T^{nm}. One is thus led to ascribe this finding to the long-range nature of the interaction carried by the pion which, on the one side, can sustain a collective motion even in a rarefied medium and, on the other hand, keeps a substantial strength even at quite short wavelengths.

To ascertain whether the p-h excitations remain confined on the surface or spread out inside the nucleus, one should modify, the present formalism by inserting propagators of the type $\hat{\Pi}^{ss}$ everywhere in (2.1).

VI. CONCLUSIONS

In 1971 a phase transition was conjectured to occur in nuclear matter at a density of about $2\rho_0$, signalling the condensation of pions.[23,24] A layered order of nucleons in the spin-isospin space would disclose the phenomenon.

Since then, precursor phenomena of the pion condensation have been extensively searched for in atomic nuclei. In particular, the nuclear unnatural parity excited states (notably the $J^\pi=0^-$, $\tau=1$) have been thoroughly explored,[25] as the pion carried force should lower their energy. Pionic fingerprints have also been looked for[26] in a possible enhancement of the inelastic form factor of the 1^+ excited state of C^{12} at large momentum transfers.

All these researches have been essentially inconclusive. Accordingly the death, sentenced to pion condensation, was gradually extended to precursor phenomena as well: the value of g' was considered too large to allow pionic manifestations inside nuclear structure.

Nevertheless, in 1980, it was argued[27] that the spin-longitudinal isovector nuclear response in the QEP region should still reflect the action of the pion. In the words of

Siemens *et al.*[28] this suggestion is analogous to "look for the giant quadrupole resonance instead of investigating the $E2$ effective charge in the low-energy surface vibrations."

Extending this line of thought, it was later suggested[1] that the contrast between the $\sigma \cdot \mathbf{q}$ and the $\sigma \times \mathbf{q}$ isovector nuclear responses would in fact offer the best way of detecting pionic phenomena in the QEP region.

This idea prompted the Los Alamos experiment, which led to negative results. However, a variety of nuclear phenomena concur in hiding the pion, at least partly, in a (p,p′) polarized reaction. A (p,n) experiment of similar type would help in shedding light on the matter.

Then, in the (He^3,t) charge-exchange reaction, the pion finally seemed to come into the open in nuclear physics, but this conclusion clearly needs further support, before being wholly trusted. It would indeed be paradoxical that precursor phenomena of pion condensation, previously ruled out on the basis of the too low density of atomic nuclei, should manifest themselves in the nuclear surface, a region where the density is even smaller.

On the experimental side, high priority should be given to the separation of the $\sigma \cdot \mathbf{q}$ component in the (He^3,t) cross section. On the theoretical side, exact RPA calculations of the $\sigma\tau$ nuclear response in the deep inelastic region should be performed. Moreover, the validity of the one-step description of the reaction process should be assessed.

The 2p-2h excitations should also be included to achieve a really comprehensive treatment: their role has been shown to be decisive in bringing the theory close to the experiment in the volume (e,e′) transverse scattering. It is true that in a surface response only the peripheral region of the nucleus is probed and this, by itself, weakens the 2p-2h contribution; yet, the background, clearly visible in the (He^3,t) data, seems to require, at least partly, their presence.

Finally, relativity cannot be ignored at large momenta, where the most significant effect of the experiment by Bergqvist *et al.* shows up. Whether a calculation of a relativistic RPA surface response is presently feasible is, however, hard to assess.

In conclusion, many shortcomings wait for a deeper investigation; nevertheless, the argument is so exciting that the efforts for reaching a full understanding of the pion role in nuclear structure are well justified. Indeed, the spin-isospin correlations, from their spectacular appearance in the (p,n) reaction at the Indiana University Cyclotron,[29] where the GT giant resonance and the related missing strength were discovered, until the present experiments of Los Alamos and Saturne, have revealed themselves as one of the most intriguing and fascinating aspects of nuclear structure.

The authors wish to acknowledge clarifying discussions with J. Delorme, C. Gaarde, and E. Oset.

---

[1]W. M. Alberico, M. Ericson, and A. Molinari, Nucl. Phys. **A379**, 429 (1982).
[2]G. Chanfray, Nucl. Phys. **A429**, 489 (1984).
[3]T. A. Carey *et al.*, Phys. Rev. Lett. **53**, 144 (1984); L. B. Rees *et al.*, Phys. Rev. C **34**, 627 (1986).
[4]I. Bergqvist *et al.*, Nucl. Phys. **A469**, 648 (1987).
[5]W. M. Alberico, A. De Pace, M. Ericson, M. B. Johnson, and A. Molinari, Phys. Lett. **B183**, 135 (1987).
[6]R. J. Glauber, in *Lectures in Theoretical Physics,* edited by W. Brittin *et al.* (Interscience Publishers, New York, 1959), Vol. 1.
[7]T. Shigehara, K. Shimizu, and A. Arima, Nucl. Phys. **A477**, 583 (1988).
[8]Y. Okuhara, B. Castel, I. P. Johnstone, and H. Toki, Phys. Lett. B **186**, 113 (1987).
[9]H. Esbensen, H. Toki, and G. F. Bertsch, Phys. Rev. C **31**, 1816 (1985).
[10]G. Chanfray, in *International Symposium on Weak and Electromagnetic Interactions in Nuclei,* edited by H. V. Klapdor (Springer-Verlag, Berlin, 1986).
[11]G. Orlandini, M. Traini, and M. Ericson, Phys. Lett. B **179**, 201 (1986).
[12]W. M. Alberico, A. De Pace, and A. Molinari, Phys. Rev. C **31**, 2007 (1985).
[13]W. M. Alberico, A. Molinari, A. De Pace, M. Ericson, and M. B. Johnson, Phys. Rev. C **34**, 977 (1986).
[14]H. Toki and W. Weise, Phys. Rev. Lett. **42**, 1034 (1979); Z. Phys. A **292**, 389 (1979).
[15]H. Esbensen and G. F. Bertsch, Ann. Phys. (N.Y.) **157**, 255 (1984).
[16]G. F. Bertsch and O. Scholten, Phys. Rev. C **25**, 804 (1982).
[17]C. Gaarde, private communication.
[18]Z. E. Meziani *et al.*, Phys. Rev. Lett. **54**, 1233 (1985).
[19]C. Gaarde, Nucl. Phys. **A478**, 475c (1988).
[20]D. V. Bugg and C. Wilkin, Phys. Lett. **152B**, 37 (1985).
[21]W. M. Alberico, T. W. Donnelly, A. Molinari, and J. W. Van Orden (unpublished).
[22]A. Hosaka and H. Toki, Progr. Theor. Phys. **76**, 1306 (1986).
[23]A. B. Migdal, Zh. Eksp. Teor. Fiz. **61**, 2209 (1971) [Sov. Phys.—JETP **34**, 1184 (1972)]; Usp. Fiz. Nauk **105**, 781 (1971) [Sov. Phys. Usp. **14**, 813 (1972)].
[24]F. Calogero and F. Palumbo, Lett. Nuovo Cimento **6**, 663 (1973).
[25]J. Meyer-Ter-Vehn, Phys. Rep. **74**, 323 (1981); J. Speth, V. Klemt, J. Wambach, and G. E. Brown, Nucl. Phys. **A343**, 382 (1980).
[26]J. Delorme, M. Ericson, A. Figureau, and N. Giraud, Phys. Lett. **89B**, 327 (1980); H. Toki and W. Weise, *ibid.* **92**, 265 (1980).
[27]W. M. Alberico, M. Ericson, and A. Molinari, Phys. Lett. **92B**, 153 (1980).
[28]T. Izumoto, M. Ichimura, C. M. Ko, and P. J. Siemens, Phys. Lett. **112B**, 315 (1982).
[29]C. Goodman, Nucl. Phys. **A396**, 127c (1982).
[30]These figures hold valid at 515 MeV; presumably no dramatic change takes place between 515 and 667 MeV.